2014

Dynamic fracture analysis of polycarbonate by the optical method of caustics

Guiyun Gao
Peking University

Zheng Li
Peking University, lizheng@pku.edu.cn

Mehrdad Negahban
University of Nebraska-Lincoln, mnegahban1@unl.edu

Available online at www.sciencedirect.com

ScienceDirect

Procedia Materials Science 3 (2014) 165 – 176

Procedia Materials Science

www.elsevier.com/locate/procedia

20th European Conference on Fracture (ECF20)

Dynamic fracture analysis of polycarbonate by the optical method of caustics

Guiyun Gao[a], Zheng Li[a,*], Mehrdad Negahban[b]

[a]*State Key Lab for Turbulence and Complex Systems and College of Engineering, Peking University, Beijing 100871, PR China*
[b]*Department of Engineering Mechanics, University of Nebraska-Lincoln, Lincoln, NE 68588, USA*

Abstract

Glassy polycarbonate (PC) is a widely used engineering material in industries, since it has high strength and toughness as well as good transparency. However, these advantages of PC can be suppressed by physical aging, especially its dynamic fracture toughness. In addition, the material properties of PC can be changed dramatically after large plastic compressive deformation, and it can show obvious orthotropic behavior. Here, the combined effect of aging and plastic compressive deformation on dynamic facture of PC was investigated by the optical method of caustics. The dynamic reflective method of caustics for orthotropic materials was developed here to study the dynamic fracture property of PC with plastic deformation. The samples were prepared with different extents of plastic compressive strain up to approximately 50% engineering strain, followed by aging with various aging times up to 300 hours. The shadow spot patterns during the fracture processes were recorded by a high speed camera. Results show that the PC with plastic compressive deformation has different fracture toughness even quite different fracture modes on its different orientations. Aging affects the fracture property of PC with or without plastic flow in similar trend. Under large plastic compressive strain, PC has more strong anisotropy and dynamic fracture tolerance, which has great potential for optimal material design.

Selection and peer-review under responsibility of the Norwegian University of Science and Technology (NTNU), Department of Structural Engineering

* Corresponding author. Tel.: +86-10-62754624; fax: +86-10-62751812.
E-mail address: lizheng@pku.edu.cn

Selection and peer-review under responsibility of the Norwegian University of Science and Technology (NTNU), Department of Structural Engineering
doi:10.1016/j.mspro.2014.06.031

Keywords: Polycarbonate; Physical aging; Plastic strain; Fracture toughness.

1. Introduction

Polycarbonate (PC) plays a vital important role in engineering application (such as windshields, protective eye wear, bullet-proof glass, and blast barriers) due to its superior impact resistance. However, the mechanical properties of PC, especially the fracture properties, strongly depend on its thermal and mechanical history. That is the physical aging and plastic deformation could cause changes in mechanical properties of glassy polycarbonate (PC).

Many works are devoted to study the aging effect on mechanical properties, such as tensile strength and creep behavior (Senden et al. (2012), Sakai and Somiya (2011)). Ho et al. (2004) considered the effect of aging on the fracture properties of PC by using the essential work of fracture (EWF) method. However, EWF parameters can mislead in understanding fracture behavior and cannot be used to characterize fracture performance. Large plastic deformations in some glassy polymers may induce substantial change from isotropic material into anisotropic one. And the anisotropy of PC with plastic flow could be observed in the difference of Young's modulus by Goel (2009). Although the individual effects of physical aging and plastic flow have been studied, limited work deals with the combined effects on the mechanical properties especially the dynamic fracture behaviors of PC with large plastic strains. Group in University of Nebraska-Lincoln has investigated this combined effect of physical aging and plastic flow by Charpy impact, quasi-static Single Edged Notched Bending (SENB) and Compact Tension (CT) tests (Meagher (2010). However, these methods cannot cope with anisotropic fracture, and the dynamic fracture process cannot be depicted using these conventional fracture testing methods.

The method of caustics is one of the most important experimental methods in fracture mechanics, which is extended to study fracture problems of various materials with viscoelastic or plastic properties (Gao et al. (2011), Unger (2005)). Since Lee et al. (1996) derived the dynamic stress field and dynamic displacement field around the crack tip of an orthotropic material, the application of caustic method in anisotropic material is possible. Then Gong et al (2008) developed this method to study the dynamic fracture problems of carbon fiber reinforced composite materials. Therefore, the optical method of caustics is chosen to investigate the dynamic fracture behavior of aged and plastic compressed PC in this paper.

In this paper, the combined effects of aging and plastic flow on dynamic fracture property of PC are investigated by using the reflective dynamic method of caustics. The relation between caustic curve and stress intensity factor was deduced first. Then the dynamic fracture tests were conducted by three points bending beam impacted by drop weight. The caustic patterns during the dynamic fracture process were recorded by a high speed camera, and the dynamic fracture parameters are determined from the patterns. Finally, the aging and plastic flow effects are discussed.

Nomenclature

a	crack length
d	thickness of specimen
$[C_{ij}]$	components of stiffness tensor
D_t	diameter of caustic curve
K_I, K_{II}	dynamic stress intensity factors for mode I and mode II cracks
K_{IC}	critical stress intensity factor of mode I
$[s_{ij}]$	compliance material matrix of orthotropic composite
x, y	coordinates of rectangular coordinate system
z_0	distance from reference plane to specimen
λ_m	scale factor which equals to 1 for parallel light
ρ	density of PC
c	crack moving speed
σ_x, σ_y, τ_{xy}	stress components

2. Method of caustics for orthotropic materials

For the transparency of processed PC by thermal aging or plastic compression is not sufficient for transmiting light rays in good quality, the reflective method of caustics is adopted. When a specimen is loaded, the thickness around crack tip will be changed obviously since the strong strain singularity. If a parallel light rays incident on the surface of specimen, the reflected light beams around crack tip will deflect the light path dramatically. These light beams can transfer from the specimen surface to a virtual plane at a distance z_0 behind the specimen, and a singular caustic curve (concentrated light around a dark spot) can be seen if a camera is set with focus on this virtual plane. According to the geometrical optical principle, if we set the crack tip as the original point and x axis along the crack direction, a point $P(x, y)$ on the specimen surface can be mapped at the point $P'(x',y')$ on the virtual plane as (Gong et al. (2008))

$$\vec{r}\,' = \lambda_m \vec{r} - z_0 d\,\mathrm{grad}\left(s_{31}\sigma_x + s_{32}\sigma_y + s_{31}\tau_{xy}\right), \tag{1}$$

where, $[s_{ij}]$ is the compliance material matrix of orthotropic composite, λ_m is a scale factor which equals to 1 for parallel light, and d is the thickness of specimen.

The stress distribution around the crack tip for mixed mode crack opening in moving crack case is derived by Lee et al. (1996) in form

$$\sigma_x = \frac{K_I}{\sqrt{2\pi r}}\mathrm{Re}\left\{\frac{1}{(1+M_1)(\mu_1-\mu_2)}\left[\frac{\left(m_2^2+M_2\right)\mu_1}{\sqrt{\cos\theta+m_2\sin\theta}}-\frac{\left(m_1^2+M_2\right)\mu_2}{\sqrt{\cos\theta+m_1\sin\theta}}\right]\right\} + \frac{K_{II}}{\sqrt{2\pi r}}\mathrm{Re}\left\{\frac{1}{(\mu_1-\mu_2)}\left[\frac{\left(m_2^2+M_2\right)}{\sqrt{\cos\theta+m_2\sin\theta}}-\frac{\left(m_1^2+M_2\right)}{\sqrt{\cos\theta+m_1\sin\theta}}\right]\right\} \tag{2a}$$

$$\sigma_y = \frac{K_I}{\sqrt{2\pi r}}\mathrm{Re}\left\{\frac{1}{(\mu_1-\mu_2)}\left[\frac{\mu_1}{\sqrt{\cos\theta+m_2\sin\theta}}-\frac{\mu_2}{\sqrt{\cos\theta+m_1\sin\theta}}\right]\right\} + \frac{K_{II}}{\sqrt{2\pi r}}\mathrm{Re}\left\{\frac{(1+M_1)}{(\mu_1-\mu_2)}\left[\frac{1}{\sqrt{\cos\theta+m_2\sin\theta}}-\frac{1}{\sqrt{\cos\theta+m_1\sin\theta}}\right]\right\} \tag{2b}$$

$$\tau_{xy} = \frac{K_I}{\sqrt{2\pi r}}\mathrm{Re}\left\{\frac{\mu_1\mu_2}{(1+M_1)(\mu_1-\mu_2)}\left[\frac{1}{\sqrt{\cos\theta+m_1\sin\theta}}-\frac{1}{\sqrt{\cos\theta+m_2\sin\theta}}\right]\right\} + \frac{K_{II}}{\sqrt{2\pi r}}\mathrm{Re}\left\{\frac{1}{(\mu_1-\mu_2)}\left[\frac{\mu_1}{\sqrt{\cos\theta+m_1\sin\theta}}-\frac{\mu_2}{\sqrt{\cos\theta+m_2\sin\theta}}\right]\right\} \tag{2c}$$

where,

$$M_1 = \rho c^2\left(s_{12}-s_{11}\right),\ M_2 = \rho c^2\left(s_{12}-s_{22}\right),$$

$$\mu_1 = m_1 - \rho c^2 s_{22} / m_1 - m_1 \rho c^2 s_{11} + \left(\rho c^2\right)^2 \left(s_{11}s_{22} - s_{12}^2\right) / m_1 ,$$

$$\mu_2 = m_2 - \rho c^2 s_{22} / m_2 - m_2 \rho c^2 s_{11} + \left(\rho c^2\right)^2 \left(s_{11}s_{22} - s_{12}^2\right) / m_2 ,$$

$$m_1 = i\sqrt{B_{12} - \sqrt{B_{12}^2 - K_{66}}} , \quad m_2 = i\sqrt{B_{12} + \sqrt{B_{12}^2 - K_{66}}} ,$$

$$B_{12} = \frac{1}{2s_{11}}\left[2s_{12} + s_{66} + \rho c^2 \left(s_{12}^2 - s_{11}s_{66} - s_{11}s_{22}\right)\right],$$

$$K_{66} = \left\{s_{22} + \rho c^2 \left[s_{12}^2 - s_{22}a_{66} - s_{11}s_{22} + \rho c^2 s_{66}\left(s_{11}s_{22} - s_{12}^2\right)\right]\right\} / s_{11} , \text{ and } K_{66} > 0 ,$$

here, ρ is the density, c is the crack moving speed. K_I and K_{II} are dynamic stress intensity factors for mode I and mode II cracks, respectively.

By inserting Eq. (2) into Eq. (1), the mapping formula can be derived. By using optical diffractive theory, the sufficient and necessary condition of singularity is that the Jacobian determinant of mapping formula is zero, namely,

$$J = \begin{vmatrix} \frac{\partial x'}{\partial r} & \frac{\partial x'}{\partial \theta} \\ \frac{\partial y'}{\partial r} & \frac{\partial y'}{\partial \theta} \end{vmatrix} = \frac{\partial x'}{\partial r}\frac{\partial y'}{\partial \theta} - \frac{\partial x'}{\partial \theta}\frac{\partial y'}{\partial r} = 0 . \tag{3}$$

Therefore, the initial curve of caustics is proposed as

$$r = (z_0 d \frac{K_1}{\lambda_m \sqrt{2\pi}})^{\frac{2}{5}} H_0 ,$$
(4)

and its corresponding caustic curve is

$$x_c' = \lambda_m^{\frac{3}{5}} \left(z_0 d \frac{K_1}{\sqrt{2\pi}} \right)^{\frac{2}{5}} \left\{ H_0 \cos\theta + H_0^{-\frac{3}{2}} \left[(-\frac{1}{2} L_1 \cos\theta - \frac{\partial L_1}{\partial \theta} \sin\theta) + \mu((-\frac{1}{2} L_2 \cos\theta - \frac{\partial L_2}{\partial \theta} \sin\theta) \right] \right\}$$

$$y_c' = \lambda_m^{\frac{3}{5}} \left(z_0 d \frac{K_1}{\sqrt{2\pi}} \right)^{\frac{2}{5}} \left\{ H_0 \sin\theta + H_0^{-\frac{3}{2}} \left[(-\frac{1}{2} L_1 \sin\theta + \frac{\partial L_1}{\partial \theta} \cos\theta) + \mu((-\frac{1}{2} L_2 \sin\theta + \frac{\partial L_2}{\partial \theta} \cos\theta) \right] \right\}$$
(5)

where,

$$H_0 = \left[-\frac{H_1}{2} + \sqrt{(\frac{H_1}{2})^2 - H_2} \right]^{\frac{2}{5}} , \ (\frac{H_1}{2})^2 \geq H_2 , H_1 = \frac{1}{4}\left(L_1 + \mu L_2\right) + \frac{\partial^2 L_1}{\partial \theta^2} + \mu \frac{\partial^2 L_2}{\partial \theta^2} ,$$

$$H_2 = -\frac{3}{2}\left[\frac{1}{4}L_1^2 - \frac{1}{2}L_1\frac{\partial^2 L_1}{\partial\theta} + \frac{3}{2}\left(\frac{\partial L_1}{\partial\theta}\right)^2\right] - \frac{3}{2}\mu\left(\frac{1}{2}L_1L_2 - \frac{1}{2}\frac{\partial^2 L_1}{\partial\theta^2} + 3\frac{\partial L_1}{\partial\theta}\frac{\partial L_2}{\partial\theta} - \frac{1}{2}L_1\frac{\partial^2 L_2}{\partial\theta^2}\right)$$
$$-\frac{3}{2}\mu^2\left[\frac{1}{4}L_2^2 - \frac{1}{2}L_2\frac{\partial^2 L_2}{\partial\theta^2} + \frac{3}{2}\left(\frac{\partial L_2}{\partial\theta}\right)^2\right]$$

,

$$L_1 = \mathrm{Re}\left[\frac{1}{E}(A_1C^{\frac{1}{2}} - B_1D^{\frac{1}{2}})\right],\ L_2 = \mathrm{Re}\left[\frac{1}{E}(A_2C^{-\frac{1}{2}} - B_2D^{-\frac{1}{2}})\right],$$

$$C = \cos\theta + m_2\sin\theta,\ D = \cos\theta + m_1\sin\theta,\ E = \mu_1 - \mu_2,\ \mu = K_{II}/K_I,$$

$$A_1 = \mu_1\left(\frac{\left(m_2^2 + M_2\right)}{1+M_1}\mu_1 s_{13} + s_{32}\right),\ B_1 = \mu_2\left(\frac{\left(m_1^2 + M_2\right)}{1+M_1}s_{13} + s_{32}\right),$$

$$A_2 = \left(m_2^2 + M_2\right)s_{13} + s_{32},\ B_2 = \left(m_1^2 + M_2\right)s_{13} + s_{32}.$$

For mode I crack, μ equals to 0 and the typical diameter of caustic curve can be expressed as

$$D_t = \lambda^{5/3}\left(z_0 d\frac{K_1}{\sqrt{2\pi}}\right)^{2/5}\delta, \tag{6}$$

where,

$$\delta = \delta_{\theta_1} - \delta_{\theta_2},\ \delta_\theta = \left[H_0\sin\theta + H_0^{-3/2}\left(-\frac{L_1}{2}\sin\theta + \frac{\partial L_1}{\partial\theta}\cos\theta\right)\right],$$

θ_1, θ_2 can be obtained through the solution to the formula $\frac{dy_c'}{d\theta} = 0$. Finally, the relation between stress intensity factor (SIF) and typical diamter of caustic curve D_t can be obtained as

$$K_1 = \frac{\sqrt{2\pi}}{z_0 d}\left(\frac{D_t}{\delta}\right)^{5/2}. \tag{7}$$

3. Orthotropy of plastic compressed PC

For orthotropic materials, there are 9 independent components in stiffness tensor, and the stress strain relation can be expressed as:

$$\sigma = C\varepsilon,\ C = \begin{bmatrix} C_{11} & C_{12} & C_{13} & & & \\ & C_{22} & C_{23} & & 0 & \\ & & C_{33} & & & \\ & & & C_{44} & & \\ & 0 & & & C_{55} & \\ & & & & & C_{66} \end{bmatrix}. \tag{8}$$

If we consider an elastic body with the following elastic properties: all directions in any plane perpendicular to one axis are equivalent with respect to the elastic properties, i.e., the body is isotropic in these planes. Letting x_1 and x_3 be the axis perpendicular to these planes, then we have the stress strain relations as follow, respectively:

$$C = \begin{bmatrix} C_{11} & C_{12} & C_{12} & & & \\ & C_{22} & C_{23} & & 0 & \\ & & C_{22} & & & \\ & & & \frac{1}{2}(C_{22}-C_{23}) & & \\ & 0 & & & C_{66} & \\ & & & & & C_{66} \end{bmatrix} \text{ and } C = \begin{bmatrix} C_{11} & C_{12} & C_{13} & & & \\ & C_{11} & C_{13} & & 0 & \\ & & C_{33} & & & \\ & & & C_{44} & & \\ & 0 & & & C_{44} & \\ & & & & & \frac{1}{2}(C_{11}-C_{12}) \end{bmatrix}.$$

The number of independent parameters is reduced to 5. If we incident an ultrasonic wave along the principal axis (Kazemi Najafi et al.(2005), Kriz and Stinchcomb (1979)), we have

$$\begin{bmatrix} C_{11}l_x^2 + C_{66}l_y^2 + C_{55}l_z^2 & (C_{12}+C_{66})l_x l_y & (C_{13}+C_{55})l_x l_z \\ (C_{12}+C_{66})l_x l_y & C_{66}l_x^2 + C_{22}l_y^2 + C_{44}l_z^2 & (C_{23}+C_{44})l_y l_z \\ (C_{13}+C_{55})l_x l_z & (C_{23}+C_{44})l_y l_z & C_{55}l_x^2 + C_{44}l_y^2 + C_{33}l_z^2 \end{bmatrix} \begin{bmatrix} P_x \\ P_y \\ P_z \end{bmatrix} = \begin{bmatrix} P_x \\ P_y \\ P_z \end{bmatrix} \rho v_p^2. \tag{9}$$

For example, if the incident direction is x (pre-crack direction of TT specimen), we have $l_x = 1, l_y = l_z = 0$. Then $C_{11} = \rho v_1^2\ (L), C_{66} = \rho v_2^2(T), C_{55} = \rho v_3^2\ (T)$ which could be obtained by using TA specimen. For y and z directions we also have $C_{66} = \rho v_1^2\ (T)$, $C_{22} = \rho v_2^2(L)$, $C_{44} = \rho v_3^2\ (T)$, and $C_{55} = \rho v_1^2\ (T)$, $C_{44} = \rho v_2^2(T)$, $C_{33} = \rho v_3^2\ (L)$, which could be obtained from TA and TT samples, respectively.

The PC specimens are cut with different directions, which are named TT (**T**ransversely cut and **T**ransversely crack propagation) and TA (**T**ransversely cut and **A**xial crack propagation) specimens (as listed in Table 1). And the elastic properties of TT and TA samples were tested using ultrasonic method and list in Table 1, and slightly difference could be clearly seen between different aging times and different plastic compression ratios.

Table 1 Specimen designs and their orthotropic mechanical properties.

Sample type	No.	Plastic strain	Aging time [h]	E_1 [GPa]	E_2 [GPa]	G_{12} [GPa]	ν_{23}	ν_{12}
---	T0-0%	0%	0	2.77	2.77	0.99	0.40	0.40
	T1-0%		50	2.77	2.77	1.00	0.39	0.39
	T2-0%		100	2.65	2.65	0.95	0.39	0.39
	T3-0%		300	2.80	2.80	1.00	0.40	0.40
TT	T0-25%TT	25%	0	3.37	3.64	0.98	0.47	0.31
	T1-25%TTD		2	3.46	3.46	1.22	0.39	0.42

	T1-25%TTB		2	3.34	3.34	1.22	0.46	0.36
	T2-25%TT		20	2.90	2.77	1.02	0.47	0.36
	T3-25% TT		300	2.85	2.85	0.99	0.36	0.44
	T4-25% TT		5	3.42	3.42	1.18	0.30	0.45
	T2-50%TT	50%	100	3.14	3.14	1.08	0.36	0.45
	T3-50%TT		300	3.12	3.12	1.07	0.35	0.46
TA	T0-25%TA		0	3.37	3.64	0.98	0.47	0.31
	T2-25%TAD	25%	200	3.15	2.82	1.06	0.47	0.36
	T2-25%TAB		200	3.04	3.00	1.06	0.46	0.35
	T3-25%TA		300	2.96	2.85	0.92	0.44	0.37
	T0-50%TA		0	3.25	3.67	0.99	0.48	0.29
	T1-50%TA	50%	50	2.82	3.05	0.88	0.47	0.33
	T2-50%TA		100	3.00	3.13	0.94	0.45	0.34
	T3-50%TA		300	3.12	3.17	0.96	0.49	0.32

The typical caustic curve and the initial curve derived by considering the orthotropic properties of PC are shown in Fig. 1. The initial curves of TA samples are similar to each other and the TT sample are somewhat resemble to each other and similar to isotropic materials. This does make sense because it's isotropic in plane and the deformation is uniform (TT sample), but the other direction would be different and there would have gradient (TA sample) in material properties.

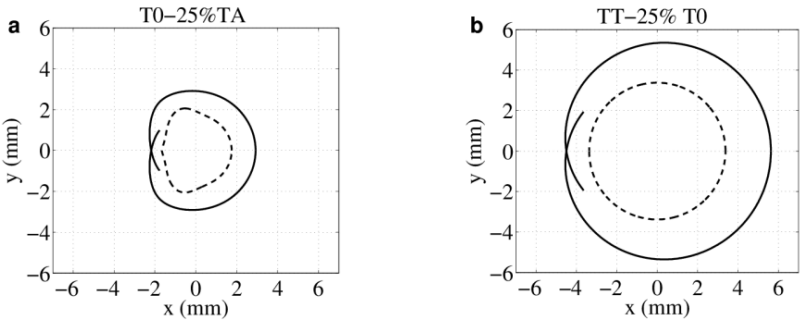

Fig. 1 The initial curves (dash line) and the caustic curves (solid line) of TA (a), and TT (b) specimens with plastic strain 25% and without aging.

4. Experimental works

The samples were not plastically deformed which are denoted here as 0% compression. Other samples were compressed uniaxially on a 20,000 kN load frame to two different plastic engineering strains (approximately 25% and 50%). The compressed samples were aged at 125 °C for various aging times. The aging was isothermal and for 0, 20, 50, 100, or 300 hours at 125 °C, followed by an air quench to room temperature. After aging, they were cut and polished into samples with the dimension of 2.5mm×10mm×40mm along desired orientations.

The reflective method of caustics was adopted due to the poor transparency of samples after mechanical process, so a thin aluminum film attached on the surface of specimen by a film-transfer technology. The thickness of this thin film is just tens micrometers and can be neglected in our tests. The optical setup is schemed as Fig. 2, and the distance z_0 from the reference plane to specimen is set 430 mm. Three point bending test was chosen in our experiment. A drop hammer with 0.88 kg weight and 370 mm height was used to impact the sample. There is an edge pre-crack of 2mm at the center of beam.

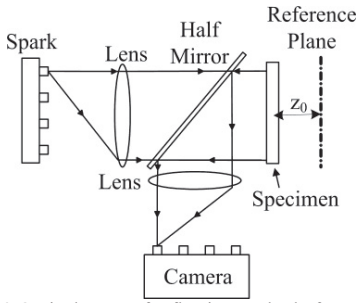

Fig. 2 Optical setup of reflective method of caustics.

5. Dynamic fracture results of anisotropic PC

5.1. Caustic patterns of orthotropic PC

The caustic patterns in the dynamic process could be captured using our high speed camera system based on the optical setup in Fig. 2. The size of the dark spot pattern changes with time as shown in Fig. 3. It means the change of specimen thickness around crack tip which is induced by the stress concentration. And with the increase of stress concentration, the caustic pattern increases and reaches its maximum value until the crack initiates. The fluctuation of the caustic pattern diameter appears during the crack propagates at different speeds.

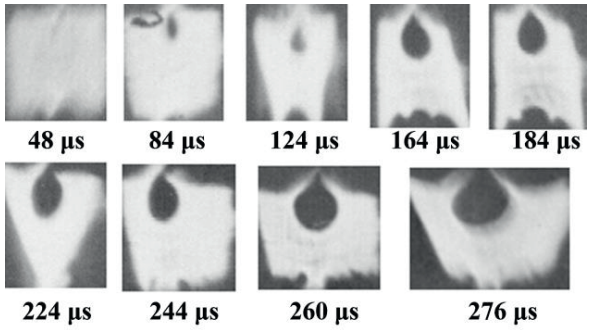

Fig. 3 Typical caustic patterns of PC. (TA-50%-T3)

The surrounding line of spot pattern is the caustic curve. Then from Fig. 3 the caustic curves are determined, and the comparison with the theoretical caustic curves obtained by Eq. (5) is shown in Fig. 4. Typical results in Fig. 4 show that they are in good agreement with the theoretical curves.

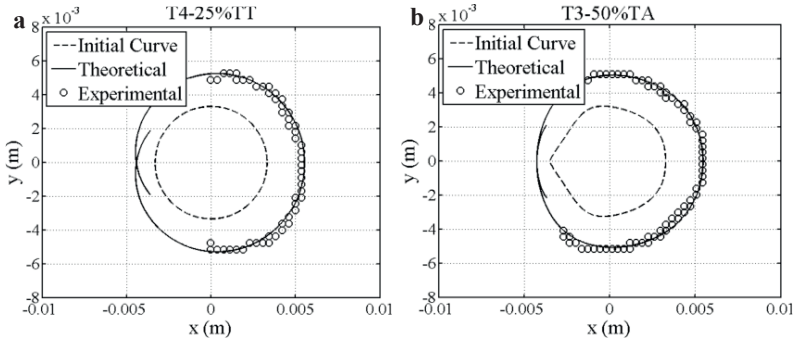

Fig. 4 Comparison of caustic curves for (a) TT, and (b) TA specimens.

5.2. Dynamic fracture parameters of PC

Once the characteristic parameters of caustic pattern are measured, the crack tip position can be determined readily. Here specimens with different aging time and plastic strain ratios are chosen. The crack length versus time during the dynamic fracture process of typical sample is shown as Fig. 5. In Fig. 5 the crack initiates at 116μs where the SIF reaches the maximum which is the critical value of stress intensity factor 17.46 MPa·m$^{1/2}$. This critical stress intensity factor corresponds to the fracture toughness. After the crack propagates, however, the SIF decreases because of the creation of new crack surface. And the crack propagation velocity is very low (about 40m/s <0.2C_R), which enhances the fracture resistance of PC. Other samples with different aging times and plastic strain ratios are similar as this typical result except for the specific values of crack initiation time and the critical value of stress intensity factors.

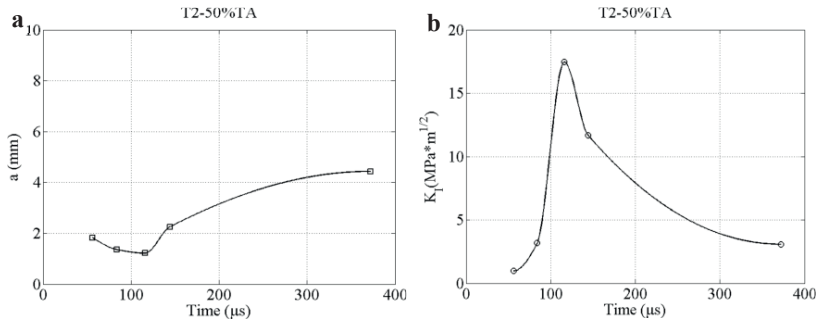

Fig. 5 Crack length versus time and stress intensity factor versus time of typical sample (No. T2-50%- TA).

5.3. Aging and plastic strain effects on dynamic fracture

Samples with different plastic compression ratios followed by physical aging were prepared and tested in dynamic method of caustics to study the aging, the plastic compression and their combined effects. The initial unaged and uncompressed samples fail in a brittle manner and have a relatively low toughness, and the critical SIF decreases with the aging time (Gao et al. (2012)). The plastic compressed samples, however, present significant difference with uncompressed ones as shown in Fig. 6. The TT samples are homogenous and isotropic in plane, which results in similar trend in TT samples with 25% plastic strain ratio. The unaged TT direction sample with plastic strain of 25% has very high critical SIF. However, the toughness decreases dramatically with aging time, and reaches the comparable value with uncompressed samples. For higher plastic compression rate, the toughness varies in the same trend as uncompressed and 25% plastic compressed ratio samples. The critical SIF of 50 % plastic strain samples are higher than that of 25% compressed or uncompressed samples. Therefore, fracture toughness of PC in TT direction increases with plastic deformation ratio.

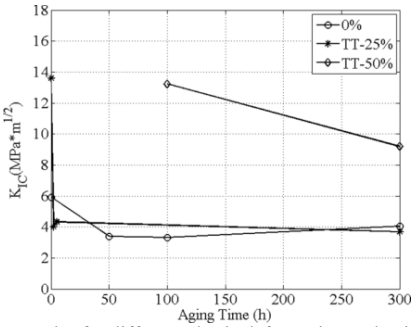

Fig. 6 TT samples for different plastic deformation and aging times.

The TA samples are quite different from specimens fabricated in other directions and their elastic properties as illustrated in Table 1. Compare with uncompressed samples, the critical SIFs are all higher and change with aging time and crack moving direction. In particular, there are two kinds of fracture mechanism in T2-25%-TA sample (shown in Fig. 7). Lower toughness indicates that specimen failures in brittle fracture and the higher one corresponds to the ductile fracture of PC. Therefore, 200 hours aging time (T2 sample) is the transition aging time of 25% compressed samples. If the plastic strain ratio increases, the toughness becomes much higher. For example, the critical SIF in 50% plastic compressed specimen is almost 15 times of uncompressed sample without aging. With the aging time increase, the toughness first decrease then a slight increase appears in TA samples of 50% plastic strain.

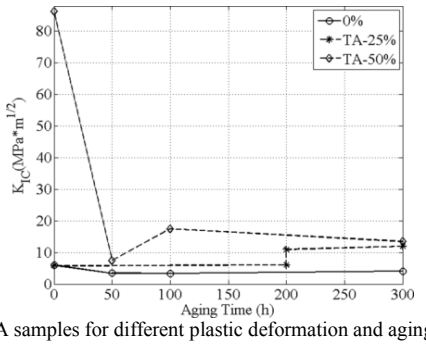

Fig. 7 TA samples for different plastic deformation and aging times.

Due to the anisotropic properties of plastic compressed PC, the toughness at different cutting direction is also different from each other. The fracture toughness of TA sample is much higher than that of TT sample with the same aging time and plastic compression ratio (as shown in Fig. 8). The changes of critical SIF with aging time, however, are in the similar trend.

It is observed, as expected and reported by Thakkar and Broutman (1981), that plastic flow without physical aging increases the fracture toughness of PC (Fig. 9). This was observed for both samples cut in the TA and TT orientations, even though the amount of increase is not the same in TA and TT samples. These results indicate that aging occurs anisotropically after plastic deformation.

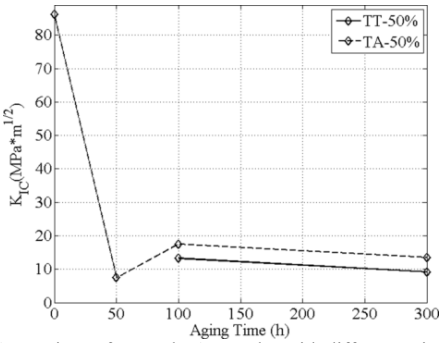

Fig. 8 Comparison of TT and TA samples with different aging times.

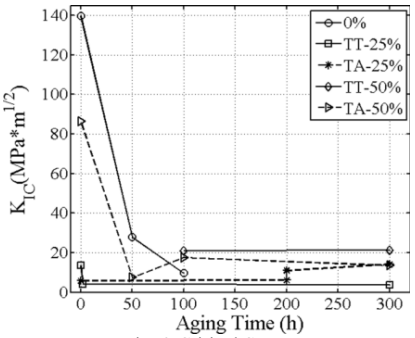

Fig. 9 Critical SIFs.

Summary

The combined effects of aging and plastic compression on dynamic facture property of glassy polycarbonate are studied by the optical method of caustics in this paper. First, thermal aging can decrease the fracture toughness of PC no matter if it is compressed with plastic flow or not. Plastic compression strain, however, can enhance the fracture toughness of PC effectively, even it can change PC's fracture behavior from brittle to ductile. Due to the anisotropy of plastic compressed PC, the fracture behavior of PC depends on the crack moving direction. Along the compression direction, the fracture tolerance can be improved much more dramatically than the crack moving direction perpendicular to the compression direction. So, PC can be designed with a perfect fracture resistance along the desired direction by plastic compression process. Therefore, these results obtained in this paper could provide a guideline for the design of functional homogenous anisotropic materials.

Acknowledgements

This work was financially supported by the National Basic Research Program of China (973Program) (No. 2010CB731503).

References

Gao, G., Li, Z. ,Negahban, M., 2012. Dynamic fracture analysis of aged glassy polycarbonate by the method of caustics. Acta Mechanica Solida Sinica.

Gao, G. Y., Li, Z. ,Xu, J., 2011. Optical method of caustics applied in viscoelastic fracture analysis. Optics and Lasers in Engineering 49**,** 632-639.

Goel, A. K., 2009. Thermodynamically consistent large deformation constitutive model for glassy polymers. Master of Science MS Thesis, University of Nebraska - Lincoln.

Gong, K. ,Li, Z., 2008. Caustics method in dynamic fracture problem of orthotropic materials. Optics and Lasers in Engineering 46**,** 614-619.

Ho, C. H. ,Vu-Khanh, T., 2004. Physical aging and time–temperature behavior concerning fracture performance of polycarbonate. Theoretical and Applied Fracture Mechanics 41**,** 103-114.

Kazemi Najafi, S., Bucur, V. ,Ebrahimi, G., 2005. Elastic constants of particleboard with ultrasonic technique. Materials Letters 59**,** 2039-2042.

Kriz, R. D. ,Stinchcomb, W. W., 1979. Elastic moduli of transversely isotropic fibers and their composites. Experimental Mechanics 19**,** 41-49.

Lee, K.-H., Hawong, J.-S. ,Choi, S.-H., 1996. Dynamic stress intensity factors KI, KII and dynamic crack propagation characteristics of orthotropic material. Engineering Fracture Mechanics 53**,** 119-140.

Meagher, S. E., 2010. Anamalous loss of toughness of work toughened polycarbonate. Master of Science MS Thesis, University of Nebraska - Lincoln.

Sakai, T. ,Somiya, S., 2011. Estimating the creep behavior of polycarbonate with changes in temperature and aging time. Mechanics of Time-Dependent Materials 16**,** 241-249.

Senden, D. J. A., Engels, T. a. P., Sontjens, S. H. M. ,Govaert, L. E., 2012. The effect of physical aging on the embrittlement of steam-sterilized polycarbonate. Journal of Materials Science 47**,** 6043-6046.

Thakkar, B. S. ,Broutman, L. J., 1981. mpact strength of polymers. 3: The effect of annealing on cold worked polycarbonates. Polymer Engineering and Science 21**,** 155–162.

Unger, D. J., 2005. Perfectly plastic caustics for the opening mode of fracture. Theoretical and Applied Fracture Mechanics 44**,** 82-94.